Quantum computation with superconducting charge qubits

Maxwell Ledlie

Abstract. An important advance in 20th century physics was the realisation that quantum mechanics could allow for the design of algorithms that solve certain important problems exponentially faster than any classical computer. The design of a "quantum computer" that could perform such algorithms has become a major international research interest, with a wide range of different physical implementations suggested. This article evaluates the success of one such implementation - that of superconducting quantum circuits using charge qubits - by comparing it with a set of criteria for quantum computers set out by David DiVincenzo.

1. Introduction

1.1. Motivation for quantum computation

Peter Shor in 1994 invented an algorithm that used the quantum Fourier transform to find the prime factors of integers, a task which would take a classical computer longer than the lifetime of the universe for numbers of the size typically used in practical applications [1, 2]. Such an algorithm has profound implications for information security. Almost all information that is currently exchanged over the internet is kept secure using *RSA encryption* [3]. While the details of this method are beyond the scope of this article, a brief summary will highlight the importance of quantum computers: All cryptosystems involve a *key*, which can be used to decode the message. RSA cryptography uses both a *public key*, which is available to anyone, and a *private key*, which is only known by the sender. The public key is an extremely large integer, and the private key is obtained from the prime factors of the integer. The security of RSA encryption relies on the fact that it is a very easy problem (multiplication) to obtain the public key from the private key, but a very hard problem (prime factorisation) to obtain the private key from the public key. The efficiency of quantum computers at prime factorisation therefore makes them a highly disruptive technology, as a new schema for internet security would have to be invented if such computers became available.

In a talk on computational physics given in 1982, Richard Feynman described a "universal quantum simulator" that could imitate many quantum mechanical systems, such as the interactions between atoms and molecules at high energies [4].

As well as doing things classical computers could never do, there are certain common tasks that classical computers perform regularly that could be carried out much faster by a quantum computer. For example, a standard computing task is to search a list of N elements for an entry that matches certain criteria. A classical computer can only examine one entry at a time, so takes a time proportional to N to accomplish the task. Lov Grover in 1996 devised a quantum algorithm that could perform the task in a time proportional to $\sqrt{N}$, saving vast amounts of time for large lists.

1.2. The DiVincenzo Criteria

In an influential paper in 2000, David DiVincenzo outlined five requirements that a system must fulfill in order to be considered a quantum computer, as well as two more for quantum communication [5]. While some modifications to these criteria have been suggested [6], they still provide a good filter for determining whether a proposed implementation has merit. The first five criteria are listed below, slightly modified from their original wording, and in a different order than that by DiVincenzo:

(i) A scalable physical system with well characterised qubits.
(ii) A universal set of quantum gates.
(iii) The ability to intialise the state of the qubits to a simple intitial state.
(iv) Long relevant decoherence times, much longer than the gate operation time.
(v) A qubit-specific measurement capability.

In the main body of this article, each of these criteria are discussed in turn. For each criterion, the abstract theory is introduced, and then specific superconducting implementations are discussed.

2. Qubits

2.1. Theory of qubits

The first DiVincenzo criterion is "a scalable physical system with well characterised qubits". We must first define a *qubit*. The unit of information in classical computation is the *bit*. This is represented by a system which can take on one of two states, denoted *0* and *1*. In modern classical computers, the system used is almost always a transistor. A voltage across the transistor that is greater than some critical value represents a 1, and a voltage less than that indicates a 0 [7]. The analogous concept to the bit in quantum computation is the 'quantum bit', or *qubit*. While a classical bit can hold only one of the two possible values, a qubit can be in a superposition of both. That is, the general state of a qubit is

$$|\psi\rangle = \alpha\,|0\rangle + \beta\,|1\rangle\,, \tag{1}$$

where α and β are complex numbers. When the state of the qubit is measured, the probability of finding it in the $|0\rangle$ state is $|\alpha|^2$, and the probability of finding it in the $|1\rangle$ state is $|\beta|^2$. Clearly the total probability of finding it in either of these states must be unity, so we have the normalisation condition

$$|\alpha|^2 + |\beta|^2 = 1. \tag{2}$$

Geometrically, we can therefore interpret the qubit as a unit vector in a two-dimensional complex vector space:

$$|\psi\rangle = \begin{bmatrix} \alpha \\ \beta \end{bmatrix}. \tag{3}$$

The states $|0\rangle$ and $|1\rangle$ provide an orthonormal basis for this vector space, and are called *computational basis states*. Using the exponential representation of complex numbers and the normalisation condition of Equation 2, we can rewrite Equation 1 as

$$|\psi\rangle = e^{i\gamma}\left(\cos\frac{\theta}{2}|0\rangle + e^{i\phi}\sin\frac{\theta}{2}|1\rangle\right), \tag{4}$$

where θ, ϕ and γ are real numbers. The factor of $e^{i\gamma}$ has no observable effects [8], so we can ignore it, and write

$$|\psi\rangle = \cos\frac{\theta}{2}|0\rangle + e^{i\phi}\sin\frac{\theta}{2}|1\rangle. \tag{5}$$

This definition of a qubit suggests a useful geometric interpretation, where we let θ and ϕ define a point on a 2-sphere of radius 1, called the *Bloch sphere*, as shown in Figure 1.

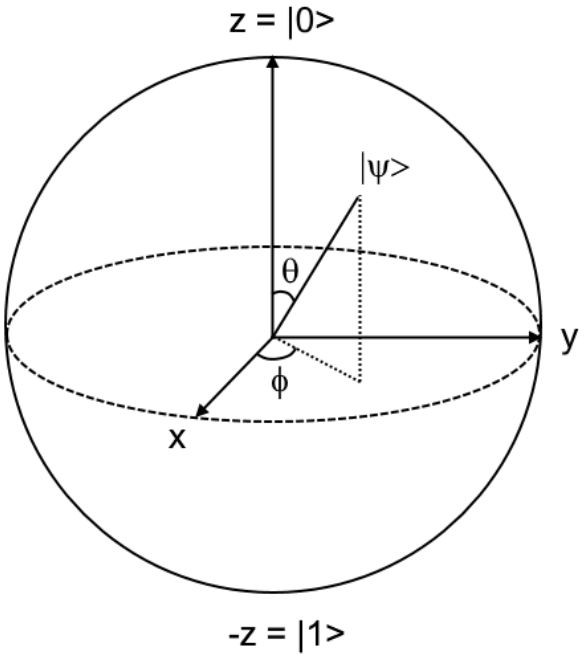

Figure 1. The Bloch sphere

In classical computing, the only allowed states are $|0\rangle$, corresponding to a vector along the z-axis, and $|1\rangle$, corresponding to a vector along the negative z-axis. (Note that this choice of directions is arbitrary. All that's required is that the directions be opposite one another.) A qubit can be represented by a vector pointing to *any* point on the surface of the sphere. The spherical polar angle θ represents the how close the state is to $|0\rangle$ or $|1\rangle$, and the azimuthal angle ϕ represents the phase of the state. A useful intuition can be gained by considering the familiar example of the spin of a spin-1/2 particle such as an electron, measured along the z-axis. Here the two basis vectors $|0\rangle$ and $|1\rangle$ in Equation 5 represent the two possible spin measurements, $\hbar/2$ ($|\uparrow\rangle$), and $-\hbar/2$ ($|\downarrow\rangle$), respectively. The direction of the state vector $|\psi\rangle$ on the Bloch sphere corresponds to the actual direction of the electron's spin state vector before it is measured and collapses to either 'up' or 'down' along the z-axis. For other two-state systems, such as the superconducting qubits we describe in the next section, the fact that the basis states aren't physical directions makes the connection between the Bloch sphere and the physical system a little less intuitive, but still just as useful mathematically.

2.2. Superconducting qubits

First discovered in 1911 by the Dutch physicist Heike Kamerlingh Onnes [9], superconductivity is a phenomenon whereby the resistivity in certain metals suddenly drops to zero as the metal is brought below some *critical temperature* T_c, which depends on the material. This was first observed in solid mercury, but has now been seen in a range of metals, such as lead and aluminium. It has been discovered that the exotic behaviour of superconductors makes them a candidate for building quantum computers. To see why this is the case, it is necessary to understand what is going on in superconductors at the microscopic level.

2.2.1. BCS Theory John Bardeen, Leon Cooper and John Robert Schrieffer proposed a microscopic explanation for superconductivity that involves the condensation of electrons into pairs [10]. In their model, electrons passing near to ions in the metallic lattice cause the ions to vibrate. The vibrational energy is transferred to adjacent ions, and the vibration travels through the lattice in the form of a quasiparticle called a phonon, which is at some point absorbed by another electron. This exchange of phonons couples the electrons, reducing their energy slightly and meaning they can together be thought of as a single quasiparticle called a Cooper pair. Individual electrons have spin 1/2, so are fermions, and obey the Pauli exclusion principle and can't occupy the same state as one another. However, the spin of a Cooper pair is the sum of the spins of its constituent electrons, i.e 1, so it behaves like a boson. So the Cooper pairs don't obey the exclusion principle, and they all condense into one macroscopic quantum state that describes the entire superconductor. This allows atomic-scale quantum phenomena to be observed at a macroscopic level. Bardeen, Cooper and Schrieffer were awarded the Nobel Prize in 1972 for their theory. It's important to highlight the advantage superconductivity gives over classical conductors. Sufficiently small samples of *any* bulk conductor will see its continuous electron conduction band turn into discrete energy levels. The difference is that the electrons all have their own microscopic quantum states, which rapidly decohere on exposure to the environment. The single macroscopic state that describes a small

section of superconductor, meanwhile, has macroscopic degrees of freedom and so has better coherence [11].

2.2.2. Superconductors and atoms At this point, it's helpful to point out an analogy between small superconductors, and natural atoms. They both have discrete energy levels, and can exhibit coherent quantum oscillations between these energy levels. These oscillations are known as *Rabi oscillations* and are discussed in Section 3.2.1. The two differ in the method used to excite transitions between energy levels. While electrons in natural atoms are excited by photons of the appropriate frequency, their superconducting equivalents are excited by currents, voltages or microwave photons, depending on the particular setup. These induce electric or magnetic fields, which affect the rate of Cooper pair tunneling across Josephson junctions [11]. Superconducting "atoms" have the advantage of being modifiable.

2.2.3. The Josephson Junction The Josephson Junction (JJ) is the key element of most superconducting quantum circuits. It consists of two sections of superconducting material separated by an insulator, as shown in Figure 2.

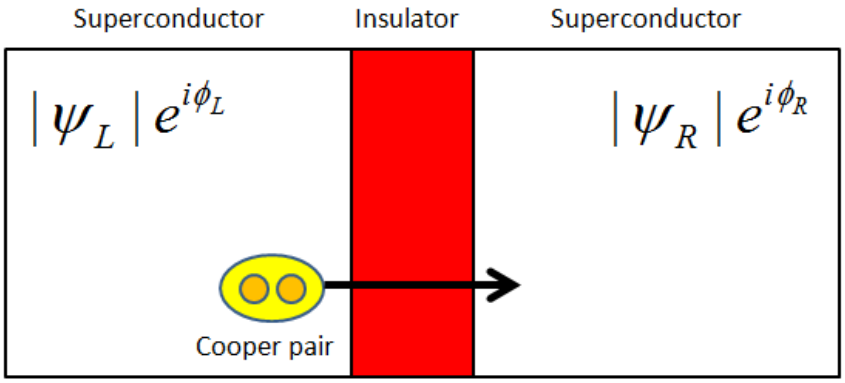

Figure 2. A Josephson Junction

The insulator creates a potential barrier between the two superconducting sections. Cooper pairs on one side of the barrier have some finite probability of quantum-mechanically tunneling across the barrier. This probability decays exponentially as the width of the barrier increases. This results in two separate wave-functions with different amplitudes and phases on either side of the junction. The basic equations governing the tunneling of Cooper pairs across the junction are [12]

$$V(t) = \frac{\hbar}{2e}\frac{\partial\phi(t)}{\partial t}, \qquad I(t) = I_C \sin(\phi(t)), \tag{6}$$

where $V(t)$ and $I(t)$ are, respectively, the voltage and supercurrent across the Josephson junction, $\phi(t)$ is the phase difference across the JJ, and I_C is the *critical*

current, the maximum supercurrent that the junction can sustain. The junction also acts as a capacitor of capacitance C. Josephson Junctions are relatively inexpensive to manufacture. They are typically made from aluminium, and the central section is allowed to oxidise, which destroys its superconducting properties and causes it to act as an insulator [13]. The critical temperature for aluminium is 1.2 K, so the components must be supercooled for the duration of the computation. Josephson junctions are crucial because they are the only electronic circuit elements that are both non-linear and non-dissipative at the low temperatures required for superconductivity [14]. The nonlinearity of Josephson junctions is important as it allows unequal spacing between energy levels, allowing the two lowest states that characterise a qubit to have a much higher probability of occupation than any higher levels. Non-dissipation is essential to reduce the rapid decoherence that would arise from any resistance in the circuit. Josephson junctions are characterised by two energy scales, E_J and E_C. E_J is the *Josephson coupling energy*, given by $E_J = I_C\Phi_0/2\pi$, where I_C is the critical current of the junction, and $\Phi_0 = h/2e$ is the magnetic-flux quantum. E_C is the *charging energy* for a Cooper pair, given by $E_C = (2e)^2/2C$, where C is the capacitance of the Josephson junction. The phase ϕ of the Cooper-pair wavefunction describing the Josephson junction, and the number n of Cooper pairs in the state, are conjugate variables, and so obey an uncertainty relation

$$\Delta n \Delta\phi \gtrsim \hbar. \tag{7}$$

With the Josephson junction acting as the basic component, three main types of superconducting qubit have been implemented, which are discussed in Sections 2.2.4 to 2.2.6. These are characterised by the ratios E_J/E_C, and $\Delta n/\Delta\phi$. Flux and phase qubits have $EC \ll E_J$, and have ϕ well-defined but allow n to fluctuate.. Charge qubits, which we focus on, have $E_C \gg E_J$, and have n well-defined but allow ϕ to fluctuate.

2.2.4. Charge qubit A charge qubit is composed of a large superconducting reservoir, which contains an effectively infinite number of Cooper pairs, separated by a Josephson Junction from a nanometre-scale superconducting box known as a *Cooper-pair box* [13], shown in Figure 3.

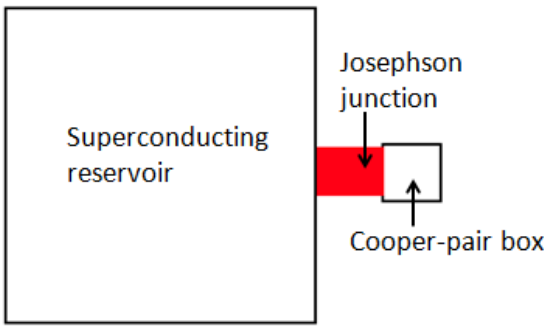

Figure 3. A Cooper-pair box

The box is small enough that it takes an appreciable amount of energy to add a single extra Cooper pair to the box. The number of pairs in the box acts as the qubit for the system, with n pairs representing the $|0\rangle$ state and $n+1$ pairs representing the $|1\rangle$ state. Due to its geometry, the Josephson junction also acts as a capacitor, with capacitance C_g. Therefore, a *bias voltage* V_g across the junction will induce a charge $Q = C_g V_g$ on either side of the junction. So we have a number of Cooper pairs $n_g = C_g V_g / 2e$ in the box, where e is the electron charge. The Hamiltonian of the system is

$$H = \sum_n 4E_C(n_g - n)^2 \left|n\right\rangle \left\langle n\right| - \frac{E_J}{2} \sum_n (\left|n\right\rangle \left\langle n+1\right| + \left|n+1\right\rangle \left\langle n\right|), \tag{8}$$

where n is an integer number of Cooper pairs. By varying the bias voltage V_g, an experimenter can control n_g, and tune this Hamiltonian. The second term in the Hamiltonian is proportional to the Josephson coupling energy E_J, and represents transitions between states of well-defined numbers of Cooper pairs - that is, quantum tunneling of Cooper pairs into and out of the box. When we ignore such quantum properties of the junction by setting E_J to 0, the Hamiltonian defines a series of parabolas with zeroes at $n_g = 1, 2, \cdots$. Neighbouring parabolas intersect at $n_g = 1/2, 3/2, \cdots$, as shown by the red lines in Figure 4 [15].

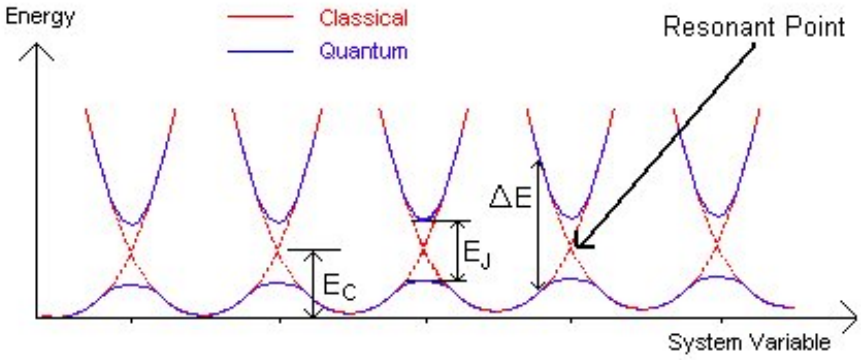

Figure 4. Energy landscape for a charge qubit. Source: Ref. [15]

The point of intersection is called the *resonant point*. Classically, the energy levels of the system cross at this point and the ground state and first excited state are degenerate, meaning the system has a well-defined energy. However, when we consider quantum effects by turning on the Josephson coupling energy E_J, the degeneracy is lifted, as shown by the purple lines in Figure 4, the energy bands are separated, and the system occupies a quantum superposition of the two energy states at the resonant point. Since the whole energy spectrum is periodic, we can choose to work only in the vicinity of the first two charge states $|0\rangle$ and $|1\rangle$, giving the simpler Hamiltonian

$$H = -\frac{1}{2}\delta E(n_g)\sigma_z - \frac{1}{2}E_J\sigma_x, \tag{9}$$

where $\delta E(n_g) \equiv 4E_C(n_g - 1/2)$ is the difference in energy between the $|0\rangle$ and $|1\rangle$ states, and σ_x and σ_z are Pauli matrices. The two eigenstates of this Hamiltonian are

$$\begin{aligned} |g\rangle &= \sin\theta/2\,|0\rangle + \cos\theta/2\,|1\rangle \\ |e\rangle &= \cos\theta/2\,|0\rangle - \sin\theta/2\,|1\rangle \end{aligned} \tag{10}$$

where $|g\rangle$ and $|e\rangle$ are the ground and excited states, and

$$\theta = \arctan E_J/\delta E(n_g). \tag{11}$$

At the degeneracy point, $\delta E(n_g) = 0$, so $\theta = \pi/2$, and

$$\begin{aligned} |g\rangle &= \frac{1}{\sqrt{2}}(|0\rangle + |1\rangle) \\ |e\rangle &= \frac{1}{\sqrt{2}}(|0\rangle - |1\rangle). \end{aligned} \tag{12}$$

That is, at the degeneracy point, the $|0\rangle$ and $|1\rangle$ states are *not* eigenstates of the system, so a system prepared in one of these states at the degeneracy point will evolve away from them and towards one of the eigenstates. We'll use this fact when we consider gate operations on a charge qubit. Experimental progress with charge qubits has been rapid. First proposed in 1997 by Shnirman et al. [16], coherent oscillations of charge qubits were observed in 1999 by Pashkin et al. [17].

2.2.5. Flux qubit A *flux qubit* is a superconducting loop interrupted by either one or three Josephson junctions, with the three-junction type more commonly implemented [18]. The computational basis states are magnetic flux pointing up through the loop, $|\uparrow\rangle$, and magnetic flux pointing down, $|\downarrow\rangle$.

2.2.6. Phase qubit The phase qubit is perhaps the least intuitive of the three types, and requires a further understanding of the dynamics of the Josephson junction. It has been shown [18] that the total potential of the junction is related to the phase difference across the junction by

$$U(\delta) = \frac{\hbar}{2e}\left(-I_C\cos\delta - I\delta\right). \tag{13}$$

This is called the *washboard potential*, and is illustrated in Figure 2.2.6 for three different values of $|I|/I_C$. The red line corresponds to the case where $|I| = I_C$, and the blue and black lines correspond to cases where $|I| < I_C$. The washboard potential has a linear dependence $-I\delta$, modulated by the *washboard modulation* $-I_C\cos\delta$. Local minima exist in this potential for $|I| < I_C$ (bias current less than critical current). The energy within each of these wells is quantised into discrete energy levels [12]. For a simple quadratic well, these energy levels would be evenly spaced, but the wells in the washboard are approximately cubic for I just less than I_C, so the spacing increases

exponentially with increasing energy level n, and this can be tuned so that only the first two energy levels can ever be expected to be occupied. These two energy levels then provide the computational basis states $|0\rangle$ and $|1\rangle$ for the system.

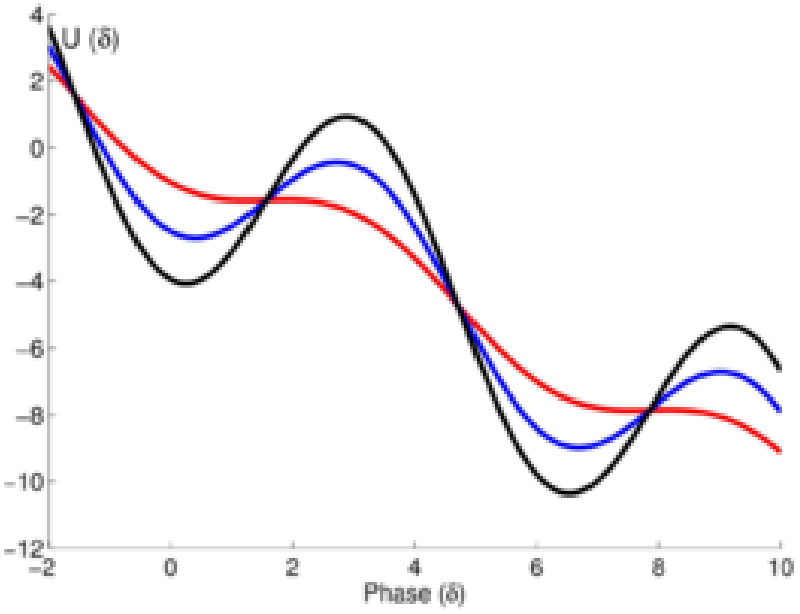

Figure 5. The washboard potential. Source: Wikipedia.

3. Quantum gates

3.1. Theory of quantum gates

The second DiVincenzo criterion is "A universal set of quantum gates". A quantum gate is an operation that can be performed on some number of qubits, with the result of changing their state. For a finite set of gates U to be "universal", we must be able to change the state of an arbitrary number of qubits to any possible state. This means that if *any* imaginable quantum computer, even one with all possible gates available to it, could perform some computation C, then C can be performed by a quantum computer using only the gate operations in U. We'll begin by looking at gate operations on single qubits.

3.1.1. Single-qubit gates In this section we follow closely the discussion by Nielsen and Chuang [8]. To understand quantum gates, it is useful to begin with a simple example. Consider the classical NOT gate, which acts on classical bits and maps $0 \to 1$ and $1 \to 0$. For the quantum analogue, we must specify not just how the gate acts on the $|0\rangle$ and

$|1\rangle$ states, but on any superposition of the two. We define the quantum NOT gate as mapping $\alpha|0\rangle + \beta|1\rangle \rightarrow \alpha|1\rangle + \beta|0\rangle$. We can represent the NOT gate with a matrix X:

$$X \equiv \begin{bmatrix} 0 & 1 \\ 1 & 0 \end{bmatrix} \tag{14}$$

Recall from Section 2.1 that a single qubit can be represented as a vector

$$|\psi\rangle = \begin{bmatrix} \alpha \\ \beta \end{bmatrix}, \tag{15}$$

where α and β are the complex amplitudes of the $|0\rangle$ and $|1\rangle$ states respectively. Then the action of a quantum NOT-gate on a qubit is represented by

$$X \begin{bmatrix} \alpha \\ \beta \end{bmatrix} = \begin{bmatrix} \beta \\ \alpha \end{bmatrix}. \tag{16}$$

This representation of qubits as vectors and gates as matrices acting on these vectors is immensely useful. Conservation of probability requires the restriction that these gate matrices U must be unitary, $U^\dagger U = I$. Considering the Bloch sphere representation of single qubits, we see that the application of the NOT gate X to a qubit is equivalent to a rotation of π around the x-axis. We can find equivalent gates for π-rotations around the y- and z-axes:

$$Y \equiv \begin{bmatrix} 0 & -i \\ i & 0 \end{bmatrix}, \quad Z \equiv \begin{bmatrix} 1 & 0 \\ 0 & -1 \end{bmatrix}. \tag{17}$$

We see that X, Y and Z are the ubiquitous *Pauli matrices*! We will often want to perform Bloch sphere rotations of some arbitrary angle, not just π. In this case we find the appropriate rotation matrix by exponentiating the relevant Pauli matrix. For example, a rotation of an angle θ around the x-axis is represented by the *rotation operator*

$$R_x(\theta) \equiv e^{-i\theta X/2} = \cos\frac{\theta}{2} I - i \sin\frac{\theta}{2} X = \begin{bmatrix} \cos\frac{\theta}{2} & -i\sin\frac{\theta}{2} \\ -i\sin\frac{\theta}{2} & \cos\frac{\theta}{2} \end{bmatrix}. \tag{18}$$

Any single-qubit gate operation - that is, movement between any two locations on the Bloch sphere - can be decomposed into rotations around two axes, along with a phase factor. More formally, if U is a unitary operation on a single qubit, then there exist real numbers α, β, γ and δ such that

$$U = e^{i\alpha} R_z(\beta) R_y(\gamma) R_z(\delta). \tag{19}$$

3.1.2. Two-qubit gates Controlling the state of a single qubit is good, but to do any interesting computations we will need to have some kind of conditional behaviour. For this we require two-qubit gates. A pair of qubits provides a four-level system, with states

$$|00\rangle, |01\rangle, |10\rangle, |11\rangle. \tag{20}$$

The pair of qubits

$$|\psi_1\rangle = \begin{bmatrix}\alpha\\ \beta\end{bmatrix}, \quad |\psi_2\rangle = \begin{bmatrix}\gamma\\ \delta\end{bmatrix} \tag{21}$$

can be represented by a single 4-dimensional vector:

$$|\psi_1\psi_2\rangle = \begin{bmatrix}\alpha\gamma\\ \alpha\delta\\ \beta\gamma\\ \beta\delta\end{bmatrix}, \tag{22}$$

which is the tensor product of the two vectors $|\psi_1\rangle$ and $|\psi_2\rangle$ [8]. The most important conditional gate in quantum computing is the *controlled-NOT*, or *CNOT* gate. It takes two input qubits - the *control qubit* $|c\rangle$ and the *target qubit* $|t\rangle$. The action of the gate is $|c\rangle\,|t\rangle \rightarrow |c\rangle\,|t \oplus c\rangle$, where the $\oplus$ operator represents addition modulo 2. That is, if the control qubit is set to $|1\rangle$ then the CNOT gate flips the target qubit. Otherwise the target qubit is unaffected. The unitary matrix representation of the CNOT gate is

$$\begin{bmatrix}1 & 0 & 0 & 0\\ 0 & 1 & 0 & 0\\ 0 & 0 & 0 & 1\\ 0 & 0 & 1 & 0\end{bmatrix}. \tag{23}$$

It can be shown [8] that any quantum gate can be approximated to arbitrary accuracy by some combination of a set of four quantum gates. They are the *Hadamard gate* H, the *phase gate* S, the $\pi/8$ *gate* T, and the CNOT gate defined above:

$$H = \frac{1}{\sqrt{2}}\begin{bmatrix}1 & 1\\ 1 & -1\end{bmatrix}, \quad S = \begin{bmatrix}1 & 0\\ 0 & i\end{bmatrix}, \quad T = \begin{bmatrix}1 & 0\\ 0 & \exp i\pi/4\end{bmatrix}. \tag{24}$$

The proof is long and is beyond the scope of this article. These four gates provide a "Universal set of quantum gates" as required by DiVincenzo.

3.1.3. Unitary operators and the Schrodinger equation We've described how we can represent gate operations as discrete unitary transformations that act on states of qubits, which we represent as vectors. This discussion seemed quite divorced from the usual Schrodinger picture of quantum mechanics, where quantum states evolve continuously over time. We'll now look at the connection between the discrete unitary operator picture and the continuous Schrödinger picture. A well known postulate of quantum mechanics is that the time evolution of the state of a closed quantum system is described by the Schrödinger equation

$$i\hbar\frac{d\,|\psi\rangle}{dt} = H\,|\psi\rangle\,, \tag{25}$$

where H is the *Hamiltonian* of the system, which is a fixed Hermitian operator. In theory, determining the Hamiltonian of a system will give complete information about its evolution. The solution to the Schrödinger equation is

$$|\psi(t_2)\rangle = \exp\left[\frac{-iH(t_2 - t_1)}{\hbar}\right]|\psi(t_1)\rangle = U(t_1, t_2)\,|\psi(t_1)\rangle\,, \tag{26}$$

where we define

$$U(t_1, t_2) \equiv \exp\left[\frac{-iH(t_2 - t_1)}{\hbar}\right]. \tag{27}$$

This operator U is clearly unitary. So we see from Equation 26 that the end result achieved by allowing a quantum state to evolve continuously under a Hamiltonian H between times t_1 and t_2 is equivalent to that achieved by applying the discrete unitary operator $U(t_1, t_2)$ defined in Equation 27 to the state. In mathematical discussions, it's usual to refer to the unitary matrices as we've done in previous sections. However, in reality, these transformations are achieved by engineering the Hamiltonian of the system to match the one appropriate for the desired transformation for the appropriate length of time. We'll see some examples of how this can be achieved in the following sections, where we discuss physical implementations of quantum gates.

3.1.4. Gate fidelity Some errors will always occur in the task of approximating unitary transformations by engineering Hamiltonians. To quantify the accuracy of unitary transformations, the *fidelity* between two quantum states ρ and σ,

$$F(\rho, \sigma) \equiv tr\sqrt{\rho^{1/2}\sigma\rho^{1/2}} \tag{28}$$

is defined as a measure of the similarity between the two states [8]. This provides a way of quantifying the accuracy of a quantum gate. For each possible input state to the gate, we can find the fidelity F between the quantum state we want to achieve by applying the gate to the input state, and the actual resultant state observed in experiment. The *gate fidelity* of a quantum gate is then defined as the worst (lowest) possible value of F across all possible input states. Gate fidelity is usually expressed as a percentage. Alternatively, the *error rate* of a gate may be more conveniently expressed, with the fidelity and error rate summing to 100%.

3.2. Superconducting quantum gates

3.2.1. Rabi Oscillations When a pulse of energy of duration Δt is applied to a two-state quantum system, the two states of the system are brought into resonance, and the system's wavefunction will coherently oscillate between the two states at the *Rabi frequency* Ω [8] [17], as shown in Figure 6. This frequency differs depending on the nature of the system and of the energy pulse, and is usually found by solving coupled differential equations. By precisely controlling the duration Δt, the final state can be chosen to be any superposition of the two states.

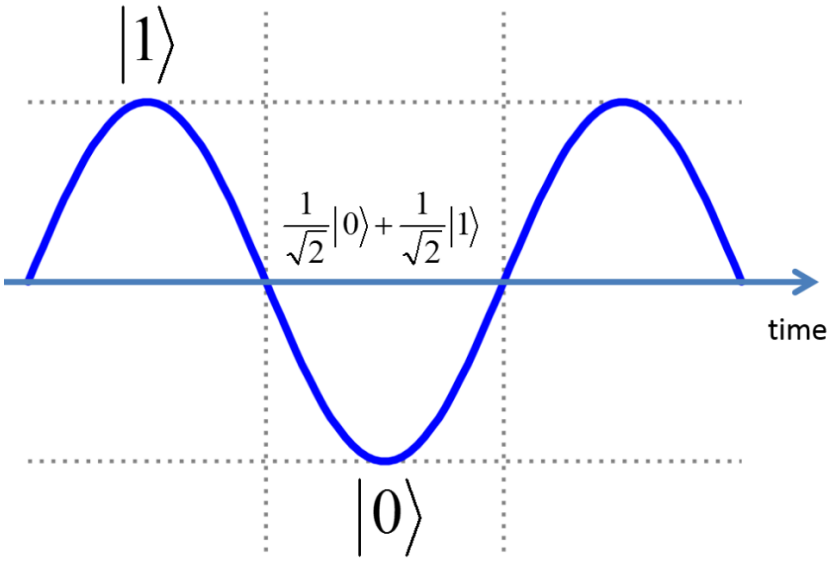

Figure 6. Rabi Oscillations

3.2.2. Single-qubit superconducting gate Just two years after the proposal of the charge qubit by Shnirman et al. [16], coherent control of a single charge qubit was demonstrated by Nakamura et al. in 1999 [17]. In addition to the constant bias voltage V_g applied across the Josephson junction as described in Section 2.2.4, they added a *pulse gate* with capacitance C_p to the Cooper pair box. Therefore the total number of Cooper pairs induced in the box was $n_g = (C_g V_g + C_p V_p)/2e$. A transmission line was connected to the pulse gate to allow for the delivery of voltage pulses as short as 80 ps. The system was prepared in the $|0\rangle$ state by choosing a bias voltage V_g to the left of the degeneracy point. A pulse was applied across the pulse gate that brought the system to the degeneracy point. As explained in Section 2.2.4, the system was now not in one of its eigenstates, so evolved according to

$$|\psi(t)\rangle = \exp -iH\Delta t/\hbar\,|0\rangle\,, \tag{29}$$

where Δt is the duration of the pulse, and H is the Hamiltonian defined in Equation 9, with $\delta E(n_g) = 0$. Solving this equation, we find that after pulse duration Δt, the probability of finding the system in state $|1\rangle$ was

$$P(1) = \frac{1}{2}\left[1 - \cos\frac{E_J \Delta t}{\hbar}\right]. \tag{30}$$

That is, the probability oscillates between 0 and 1 with period h/E_J. Here we are seeing an example of the Rabi oscillations described in Section 3.2.1, and we can have the qubit end up in any desired superposition of $|0\rangle$ and $|1\rangle$ by precisely controlling the pulse duration.

3.2.3. Two-qubit superconducting gate Coherent oscillations of a pair of coupled qubits were demonstrated by Pashkin et al. in 2003 [19], and later that year the same team used these two-qubit oscillations to implement a CNOT gate [20]. Their setup involved two charge qubits as described in Section 2.2.4, electrostatically coupled by a capacitor C_m. The two qubits were each addressed by a pulse gate and a direct current gate. The system has three characteristic energies: The Cooper-pair charging energies of the two qubits E_{c1} and E_{c2} (the energy required to add one Cooper pair to the first and second Cooper-pair boxes respectively), and the coupling energy E_m. The Hamiltonian of the system is

$$\begin{aligned} H = \sum_{n_1,n_2} & \left[E_{c1}(n_{g1}-n_1)^2 + E_{c2}(n_{g2}-n_2)^2 + E_m(n_{g1}-n_1)(n_{g2}-n_2)\right] \times |n_1,n_2\rangle\langle n_1,n_2| \\ & - \frac{E_{J1}}{2}\left[|n_1,n_2\rangle\langle(n_1+1),n_2| + |n_1,(n_2+1)\rangle\langle(n_1+1),(n_2+1)|\right] \\ & - \frac{E_{J2}}{2}\left[|n_1,n_2\rangle\langle n_1,(n_2+1)| + |(n_1+1),n_2\rangle\langle(n_1+1),(n_2+1)|\right] \end{aligned} , \tag{31}$$

where $n_1, n_2 = 0, \pm1, \pm2, \cdots$ are integer numbers of Cooper pairs, and $n_{g1,2} = (C_{g1,2}V_{g1,2} + C_P V_P)/2e$ are the number of Cooper pairs induced on the corresponding qubits by the dc and pulse gate electrodes. While the single charge qubit of Section 2.2.4 had the one-dimensional energy landscape of Figure 4, this Hamiltonian has two dimensions, n_{g1} and n_{g2}, so it defines the two-dimensional energy surface shown in Figure 7.

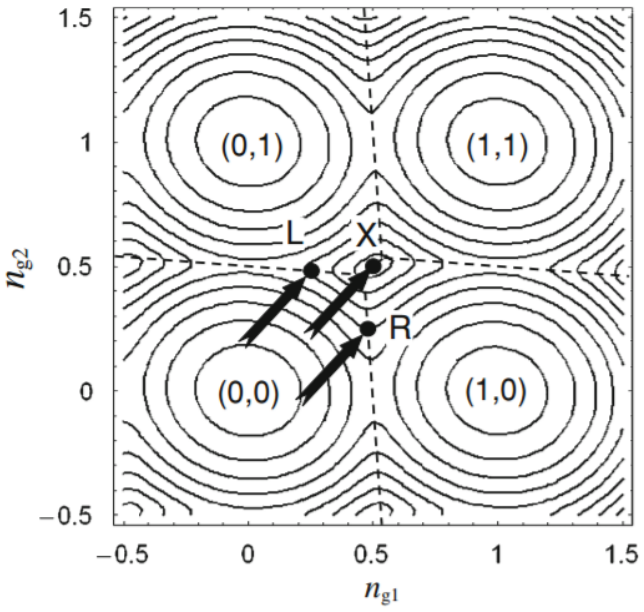

Figure 7. The energy surface of two coupled charge qubits. Source: Ref [13]. Copyright: Springer

This surface is divided into cells, each corresponding to a different charge state. The thin dashed lines indicate the degeneracy points between two different charge states, where the system is considered to be in a superposition of the states. Note that a cross-section along the n_{g1}- or n_{g2}-axes would look similar to the one-dimensional landscape of Figure 4. The marked points L and R are degeneracy points between the $|0,0\rangle$ state and the states $|0,1\rangle$ and $|1,0\rangle$ that differ by one Cooper pair in the left or right qubit respectively. There are minima in the centre of each cell, and maxima between them, with one maximum marked as X. When driven to either L or R, the system will behave like a single qubit oscillating between the degenerate states, just like in Section 2.2.4. The point X is known as a *double degeneracy point*. When brought to X, the system will oscillate between all four adjacent states. For conditional gate operation, the system is brought to somewhere along the dashed line containing L. That is, n_{g1} is fixed, and we operate along the thick dotted line in Figure 7.

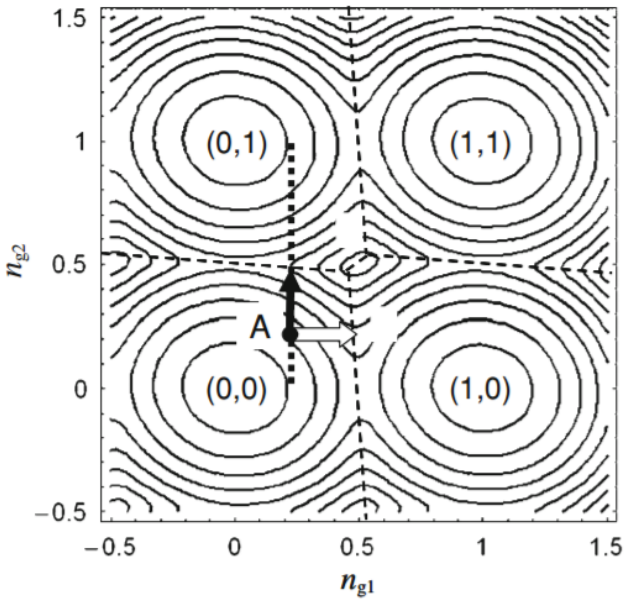

Figure 8. The pulse applied to implement a CNOT gate. Source: Ref [13]. Copyright: Springer

A voltage pulse across the second gate, indicated by the black arrow , moves n_{g2} to a degeneracy point between $|0,0\rangle$ and $|0,1\rangle$. Figure 9 shows the energy bands of the system along the thick dotted line. The four energy bands can be considered as two pairs of nearly independent single-qubit energy bands, each of which have their own degeneracy points. For the lower two bands, the control qubit is in the $|0\rangle$ state, while for the upper two bands, the control qubit is in the $|1\rangle$ state. The important point is that degeneracy occurs at slightly different values of n_{g2} between the two pairs. Therefore applying the pulse indicated below the graph in Figure 9 will bring the system to degeneracy when the system is prepared in state $|00\rangle$ or $|01\rangle$, causing oscillations between the two states, but

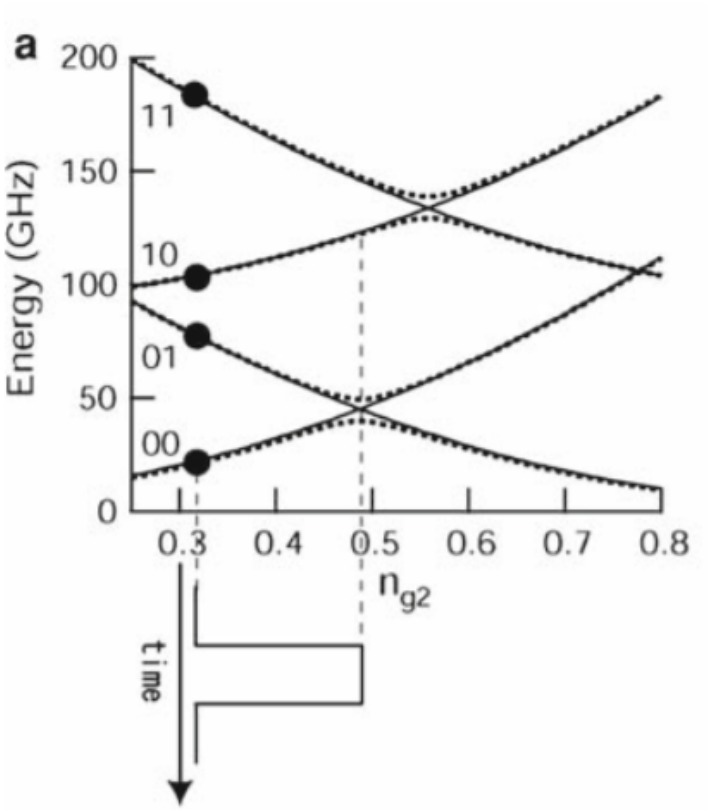

Figure 9. The four energy bands of a pair of charge qubits at degeneracy. Source: Ref [13]. Copyright: Springer.

it will *not* reach degeneracy when the system is prepared in state $|10\rangle$ or $|11\rangle$, meaning oscillations between these states are suppressed. Therefore, for a pulse of the appropriate duration and magnitude, the system will switch the second qubit only when the first qubit is 0, in accordance with the specification of a CNOT gate. A CNOT gate has also been demonstrated using flux qubits in 2007 [21].

4. Initialisation

The third DiVincenzo criterion is "The ability to initialise the state of the qubits to a simple initial state". This is analogous to the ability to reset all of the registers in a classical computer to zero, allowing the operator to begin a new computation without worrying about the contents of the registers from previous calculations causing confusion. As mentioned in Section 3.2.2, charge qubits can be set to the $|0\rangle$ state by setting the bias voltage V_g far to the left of the resonant point. So a hypothetical quantum computer based on charge qubits could be initialised by setting the bias voltage of all charge qubits to zero.

5. Decoherence

The fourth DiVincenzo criterion is "Long relevant decoherence times, much longer than the gate operation time". Much of the interesting behaviour of quantum systems arises from the fact that quantum waves interfere with one another. However, on exposure to the environment, two dangerous processes occur. The first is that the energy of the qubit is changed by its environment in an unpredictable way, bringing the qubit to thermal equilibrium with the environment on a timescale T_1 [6]. The second is that various processes will randomly change the phase of the qubit, which of course is very dangerous for quantum computing, over a timescale T_2. This phenomenon is called *decoherence*, and has been proposed as the mechanism by which the classical world emerges from the quantum. Since T_2 is almost always shorter than T_1, T_2 is the limiting factor, and is often used as a metric to compare different implementations, with larger values of T_2 being better. While we must seek to isolate qubits from their environment to reduce decoherence, there is a balancing act here, as if a qubit were completely decoupled from the environment, there would be no way to measure its state. Decoherence in a quantum computer will lead to reduced gate fidelity.

6. Measurement

The fifth DiVincenzo criterion is "A qubit-specific measurement capability". To measure the state of a charge qubit, a normal electrical lead with an ammeter can be placed near the superconducting island. A "readout" voltage pulse is then applied across the Josephson junction. This pulse is large enough to cause tunneling out of the box and into the readout lead if the box was in the $|1\rangle$ state. On the application of the pulse, the qubit will collapse to one of its eigenstates. If the qubit collapses to the $|1\rangle$ state, where there is a Cooper pair on the island, the pair will tunnel into the lead, and the ammeter will detect a current. If the qubit collapses to the $|0\rangle$ state, no current will be detected. Since the qubit can only ever be measured to be in one of its two eigenstates, no information about its previous superposition state can actually be obtained from a single readout. This doesn't matter for quantum computation though, as quantum algorithms are designed so that the final states of the readout qubits will all be eigenstates, i.e. pure $|0\rangle$ or $|1\rangle$ states, that represent the result of the computation. Pashkin et al. in 2004 [22] demonstrated such a measurement of a charge qubit.

7. Quantum error correction

In Section 3.1.4 it was mentioned that some errors will always occur in the operation of quantum gates, reducing gate fidelity. In a large quantum computer, these errors would propagate through the computer's memory. If no mechanism were in place to correct these errors, the error rate would rapidly get so high as to make the computer useless. The field of *quantum error correction* involves finding ways to correct errors in the memory of a quantum computer [23]. This is made significantly harder than for classical computers by no-cloning theorem of quantum mechanics. This theorem states that it is impossible to produce a perfect copy of an unknown quantum state. Therefore quantum data can't be protected from errors by just taking multiple copies. Furthermore, error correction must be performed without directly measuring any qubits in memory, since that would destroy the superpositions being used in computation. So

Table 1. Comparison of superconducting qubits and trapped particle qubits. Data from Ref [6].

Type of qubit	Coherence	Error rate	
	T_2	1 qubit	2 qubit
Superconducting charge qubit	4 μs	1.1%	3%
Superconducting flux qubit	4 μs	3%	60%
Superconducting phase qubit	350 ns	2%	24%
Trapped optical ion	1 ms	0.1%	0.7%
Trapped microwave ion	10 sec	0.48%	3%
Trapped neutral atoms	3 sec	5%	n/a
Liquid molecule nuclear spins	2 sec	0.01%	0.47%

researchers are faced with the daunting task of finding and correcting errors with zero information about the actual state of the qubit. Meanwhile, the field of *fault-tolerant quantum computation* seeks to develop algorithms for quantum computers that will work even in the presence of some error, provided the error is below some threshold value [24].

8. Comparison with other implementations

Superconducting quantum computation is far from the only implementation currently being investigated. For example, conditional behaviour with CNOT gates has also been demonstrated using optical qubits [25] and trapped ion qubits [26]. The main advantage of superconducting quantum computation over these other methods is scalability. Since charge qubits and Josephson junctions are solid-state circuit elements, they can easily be mass-produced, and connected to form extensive quantum computers, once decoherence can be controlled. Béjanin et al. at the University of Waterloo have in 2016 demonstrated a "quantum socket" capable of connecting as many as 100 superconducting qubits together in a three-dimensional quantum computer architecture [27]. As mentioned in Section 2.2.3, superconducting circuit elements are usually manufactured from aluminium, a relatively common and cheap material. Since superconductors are such an important material, with applications in high-end classical computing and in general materials science, further research into superconducting quantum computation is likely to be fruitful even if the end result is never a functional quantum computer. Disadvantages of superconducting quantum computing lie in the higher error rates and shorter decoherence times than in the other leading implementations. For example, Table 1 compares the the T_2 decoherence times and gate error rates of superconducting qubits with various different trapped particle qubits. It can be seen that while charge qubits are the most successful of the three superconducting qubit types, they all come up short when compared to most of the trapped particle qubits.

9. Conclusion

While a functioning, scalable, and programmable quantum computer is still a dream, astonishing progress has been made over a short period of time. The theory of quantum computation has progressed hand-in-hand with more general information theory, and the theoretical requirements to build a quantum computer are now well understood. Further progress relies on continuing to couple ever larger numbers of qubits to perform more significant computations, while maintaining insulation from the environment to minimise decoherence. Meanwhile, since decoherence will never be eradicated, the theory of quantum error correction must progress to allow larger quantum computers to operate in the presence of errors. Superconducting quantum computers have been shown to satisfy all five of the DiVincenzo criteria, and are one of the select few implementations for which a CNOT gate has actually been demonstrated. If their gate fidelity can be improved to match that of the other leading implementations, their scalability could give them a distinct advantage. However, it is far too early to commit to exclusively pursuing any one implementation. In the early days of classical computers, many different implementations of classical bits and gates were used in different contexts, from vacuum tubes and relays to the transistors that dominate today. A similar situation may arise with rudimentary quantum computers, with a variety of different implementations operating in different contexts before any single type eventually becomes prevalent.

Acknowledgements

I would like to thank my supervisors Dr Sarah Croke and Dr Thomas Brougham for their continuous support and advice throughout this project.

References

[1] Peter W. Shor. Polynomial-time algorithms for prime factorization and discrete logarithms. *SIAM J.Sci.Statist.Comput.*, 26:1484, 1997.

[2] R. J. Schoelkopf M. H. Devoret. Superconducting circuits for quantum information: An outlook. *Science*, 339:1169–1174, 2013.

[3] L. Adleman R. L. Rivest, A. Shamir. A method for obtaining digital signatures and public-key cryptosystems. *Communications of the ACM*, 21, 1978.

[4] Richard P. Feynman. Simulating physics with computers. *International Journal of Theoretical Physics*, 21, 1982.

[5] David P. Divincenzo. The physical implementation of quantum computation. 2000.

[6] T. D. Ladd et. al. Quantum computers. *Nature*, 464, 2010.

[7] Charles Petzold. *Code: The Hidden Language of Computer Hardware and Software.* Microsoft Press, 2000.

[8] I. L. Chuang M. A. Nielsen. *Quantum Computation and Quantum Information.* Cambridge University Press, 2000.

[9] J. F. Annett. *Superconductivity, Superfluids and Condensates.* Oxford University Press, 2005.

[10] L. N. Cooper & J. R. Schrieffer J. Bardeen. Theory of superconductivity. *Physical Review*, 108:1175–1204, 1957.

[11] J. Q. You & F. Nori. Superconducting circuits and quantum information. *Physics Today*, 58, 2005.

[12] S. J. Lomonaco G. Chen, L. Kauffman. *Mathematics of Quantum Computation and Quantum Technology.* Chapman & Hall, 2008.

[13] Yu. A. Pashkin et. al. Josephson charge qubits: a brief review. *Quantum Information Processing*, 8, 2009.

[14] J. M. Martinis M. H. Devoret, A. Wallraff. Superconducting qubits: A short review. 2004.

[15] S. Gildert. Introduction to qubits and quantum computing. `http://www.cm.ph.bham.ac.uk/scondintro/qubitsintro.html`. Accessed: 30/11/2016.
[16] Z. Hermon A. Shnirman, G. Schön. Quantum manipulations of small josephson junctions. *Physical Review Letters*, 79:2371–2374, 1997.
[17] Yu. A. Pashkin & J. S. Tsai Y. Nakamura. Coherent control of macroscopic quantum states in a single-cooper-pair box. *Nature*, 398:786–788, 1999.
[18] John Clarke & Frank K. Wilhelm. Superconducting quantum bits. *Nature*, 453:1031–1042, 2008.
[19] Yu. A. Pashkin et al. Quantum oscillations in two coupled charge qubits. *Nature*, 421:823–826, 2003.
[20] Yamamoto et. al. Demonstration of conditional gate operation using superconducting charge qubits. *Nature*, 425:941–944, 2003.
[21] Harmans & Mooij Plantenberg, de Groot. Demonstration of controlled-not quantum gates on a pair of superconducting quantum bits. *Nature*, 447:836–839, 2007.
[22] T. Yamamoto Y. Nakamura J. S. Tsai O. Astafiev, Y. A. Pashkin. Single-shot measurement of the josephson charge qubit. *Physical Review B*, 69, 2004.
[23] W. J. Munro & K. Nemoto S. J. Devitt. Quantum error correction for beginners. *Reports on Progress in Physics*, 76(7), 2013.
[24] D. Gottesman. An introduction to quantum error correction and fault-tolerant quantum computation. 2009.
[25] J. L. O'Brien et al. Demonstration of an all-optical quantum controlled-not gate. *Nature*, 426:264–267, 2003.
[26] T. R. Tan et al. Multi-element logic gates for trapped-ion qubits. *Nature*, 528:380–383, 2015.
[27] J. H. Béhanin et al. The quantum socket: Three-dimensional wiring for extensible quantum computing. *Physical Review Applied*, 6, 2016.